Electrochemical Differentiation of Epitope-Specific Aptamers

ARTICLE *in* ANALYTICAL CHEMISTRY · MARCH 2012

Impact Factor: 5.64 · DOI: 10.1021/ac300047c · Source: PubMed

6 AUTHORS, INCLUDING:

Mahmoud Labib
University of Toronto
33 PUBLICATIONS **612** CITATIONS
SEE PROFILE

Anna Zamay
University of Ottawa
20 PUBLICATIONS **166** CITATIONS
SEE PROFILE

John Bell
The Ottawa Hospital
225 PUBLICATIONS **11,233** CITATIONS
SEE PROFILE

Maxim V Berezovski
University of Ottawa
75 PUBLICATIONS **2,020** CITATIONS
SEE PROFILE

analytical chemistry

Article

pubs.acs.org/ac

Electrochemical Differentiation of Epitope-Specific Aptamers

Mahmoud Labib,[†] Anna S. Zamay,[†,‡] Darija Muharemagic,[†] Alexey V. Chechik,[†] John C. Bell,[§,⊥] and Maxim V. Berezovski*[,†]

[†]Department of Chemistry, University of Ottawa, 10 Marie Curie, Ottawa, Ontario K1N 6N5, Canada

[‡]Institute of Molecular Medicine and Pathological Biochemistry, Krasnoyarsk State Medical University, 1 P. Zheleznyaka str., Krasnoyarsk 660022, Russia

[§]Department of Biochemistry, Microbiology and Immunology, Faculty of Medicine, University of Ottawa, 501 Smyth Road, Ottawa, Ontario K1H 8L6, Canada

[⊥]Jennerex Inc., 450 Sansome Street, 16th floor, San Francisco, California 94111, United States

Supporting Information

ABSTRACT: DNA aptamers are promising immunoshielding agents that could protect oncolytic viruses (OVs) from neutralizing antibodies (nAbs) and increase the efficiency of cancer treatment. In the present Article, we introduce a novel technology for electrochemical differentiation of epitope-specific aptamers (eDEA) without selecting aptamers against individual antigenic determinants. For this purpose, we selected DNA aptamers that can bind noncovalently to an intact oncolytic virus, vaccinia virus (VACV), which can selectively replicate in and kill only tumor cells. The aptamers were integrated as a recognition element into a multifunctional electrochemical aptasensor. The developed aptasensor was used for the linear quantification of the virus in the range of 500−3000 virus particles with a detection limit of 330 virions. Also, the aptasensor was employed to compare the binding affinities of aptamers to VACV and to estimate the degree of protection of VACV using the anti-L1R neutralizing antibody in a displacement assay fashion. Three anti-VACV aptamer clones, vac2, vac4, and vac6, showed the best immunoprotection results and can be applied for enhanced delivery of VACV. Another two sequences, vac5 and vac46, exhibited high affinities to VACV without shielding it from nAb and can be further utilized in sandwich bioassays.

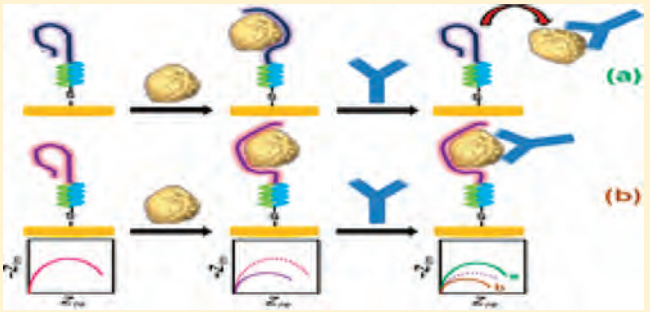

Early trace-level detection of viruses is crucial to meet urgent needs in controlling epidemics or detecting bioterrorism attacks.[1] Vaccinia virus (VACV), a member of the *Orthopoxvirus* genus of the *Poxviridae* family, served as a live vaccine to eradicate smallpox, which is caused by another *orthopoxvirus*, variola virus, in a worldwide vaccination program organized by the World Health Organization (WHO) in the last century.[2] When variola virus was eradicated in 1980, the vaccination program was stopped to prevent complications observed in a small number of vaccines.[3] Recently, there has been a renewed interest in the use of vaccinia vaccine as a defense against the deliberate release of variola virus, as an act of bioterrorism.[4] This has led to the rebuilding of vaccine stocks and created an urge for development of rapid and sensitive methods for quantifying VACV.

In addition, viral therapeutics holds a great promise for the treatment of many diseases at the cellular level.[5] VACV has a DNA genome of approximately 190 kbp and can potentially express more than 200 proteins, allowing an exceptional degree of independence from the host.[6] VACV replication and spread is associated with activation of the epidermal growth factor receptor (EGFR)-Ras signaling pathway, which is activated in most human cancers,[7] indicating that the virus could be broadly applied in cancer therapy. Oncolytic viruses (OVs) administered intravenously can be particularly effective against metastatic cancers, which are difficult to treat via conventional therapy. However, OVs can be deactivated by neutralizing antibodies (nAbs) and rapidly cleared from the circulation. Therefore, a prerequisite for successful virotherapy is that the virus must gain access to the tumor cell, which requires an extended circulation time without depletion by nAbs. The current approaches to extend the circulation time exploit polymer-coating technologies with poly-[*N*-(2-hydroxypropyl) methacrylamide][8] and polyethylene glycol[9] or preinfected T cells as carriers for delivery of oncolytic viruses to tumor sites.[10] However, these methods suffer from many drawbacks, including the permanent polymer coating of the virus leading to a loss of infectivity, whereas the latter requires the isolation of the patient's T cells and their activation followed by back-infusion, making these approaches impractical for clinical use.

Development of aptamers specific for VACV seems promising in terms of changing the viral interaction with the

Received: January 5, 2012
Accepted: February 10, 2012
Published: February 10, 2012

   dx.doi.org/10.1021/ac300047c | *Anal. Chem.* 2012, 84, 2548−2556

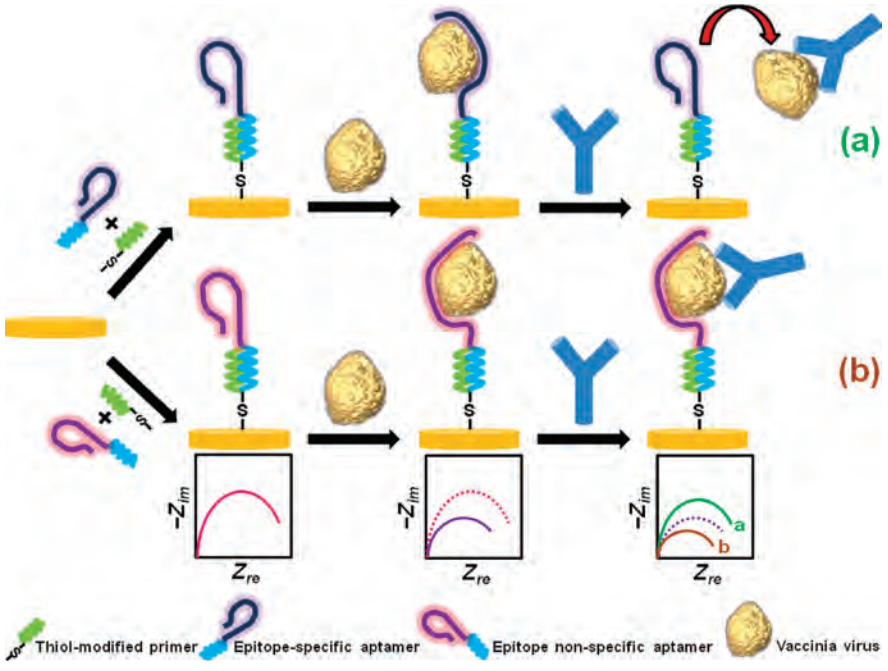

Figure 1. Schematic diagram of the electrochemical differentiation of the epitope-specific aptamers (eDEA) technique. A thiolated DNA primer is hybridized with a complementary end of a vaccinia virus (VACV)-specific aptamer (either specific or nonspecific to a viral epitope). The hybrid is self-assembled onto a gold microelectrode surface. Binding of the virus to the immobilized aptamer causes a decrease in impedance, measured by electrochemical impedance spectroscopy. Introduction of epitope-specific antivaccinia neutralizing antibody could either (a) force the virus to dissociate from the virus−aptamer complex causing a shift back in impedance in the case of an epitope-specific aptamer or (b) bind to a vacant epitope on the surface of the virus causing a further decrease in interfacial resistance if the aptamer is nonspecific to the epitope. According to the electrochemical data, all DNA aptamers can be categorized as either immunoshielding aptamers or analytical probes.

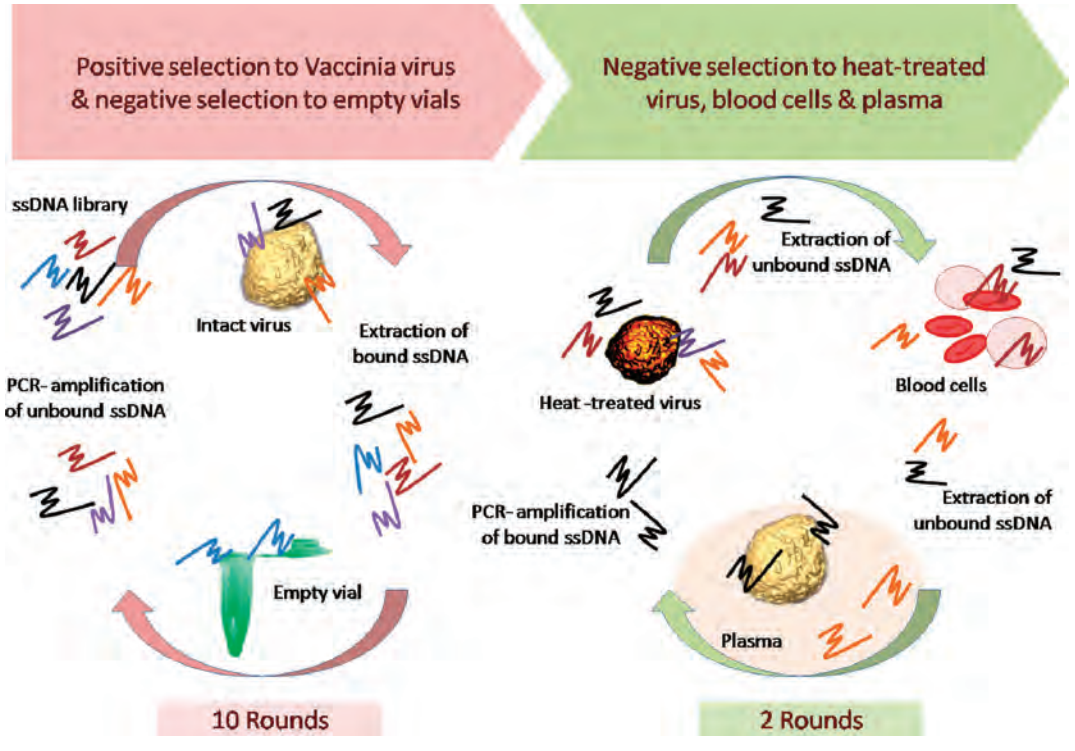

Figure 2. Scheme of DNA aptamer selection to vaccinia virus (VACV). Ten rounds of positive selection to VACV and negative selection to plastic vials includes five iterative steps: (i) incubation of VACV with a DNA library (1st round) or an aptamer pool from a previous round, (ii) partitioning of bound aptamers from unbound DNA, (iii) elimination of vial-binding DNA, (iv) heat extraction of bound aptamers, and (v) PCR amplification. Two more rounds of negative selection against inactive VACV and blood cells were combined with positive selection to VACV in the presence of blood plasma to keep nuclease-resistant aptamers.

dx.doi.org/10.1021/ac300047c | *Anal. Chem.* 2012, 84, 2548−2556

immune system. In other words, protection of the VACV surface with specific nonimmunogenic aptamers could allow the virus to escape the host immune mechanism and neutralization by the circulating antibodies. This can be feasible if the aptamers can specifically bind to the vulnerable epitopes on the virus surface. Importantly, VACV membrane is associated with at least 19 different viral proteins;[11] among them only six, A27L,[12] L1R,[13] D8L,[14] H3L,[15] A28,[16] and B5R,[17] are the targets of nAbs.

Recent reports have shown the ability of electrochemical sensors to detect several biomolecules, including proteins,[18−24] glycoproteins,[25] and carbohydrates,[26,27] with high sensitivity and excellent reproducibility. Electrochemical impedance spectroscopy (EIS) is a technique generating more and more interest for biologists as it has a less destructive effect on the measured biological interactions because it is performed at a very narrow range of small potentials and is label-free.[28,29] In the present Article, we developed a novel technology called electrochemical differentiation of epitope-specific aptamers (eDEA). It combines the selection of DNA aptamers to intact viruses and the use of a multifunctional electrochemical aptasensor for viral quantitative analysis, the estimation of aptamer binding affinity, the measurement of the degree of protection (DoP) from nAbs, and the identification of epitope-specific aptamers. As shown in the schematic presentation in Figure 1, the aptasensor is based on the formation of a self-assembled monolayer of a hybrid of a thiolated DNA capture probe and an anti-VACV aptamer as a detection probe. Electrochemical impedance spectroscopy (EIS) allows a label-free measurement of the binding event. In the following step, a high concentration of nAb is introduced and the characteristic shift in impedance allows measuring the DoP value and sorting aptamers based on their protective effect on the virus.

EXPERIMENTAL SECTION

Aptamer Selection. Aptamers were selected on the basis of cell-SELEX, an in vitro selection of nucleic acid binders to live cells, bacteria, and viruses from a random DNA library as described elsewhere.[30−33] Twelve rounds of selection against intact VACV were performed at 37 °C using the protocol schematically presented in Figure 2. First, 10 rounds of positive selection were made according to the following protocol. The selection was started with a synthetic ssDNA library (Integrated DNA Technologies, USA) which consists of a randomized region of 40 nucleotides (A/T/C/G = 25%:25%:25%:25%) flanked by two constant primer-hybridization sites, 5′-CTC CTC TGA CTG TAA CCA CG -N40- GC ATA GGT AGT CCA GAA GCC-3′. Before each round of selection and binding experiments, the ssDNA library and aptamer pools were denatured by heating for 5 min at 95 °C in Dulbecco's phosphate buffered saline, containing $CaCl_2$ and $MgCl_2$ (DPBS, #D8662, Sigma-Aldrich, USA) and then renatured on ice for 10 min. Prior to selection experiments, 2×10^{10} plaque forming units (PFU) of VACV (Jennerex Inc., Ottawa, Canada) were washed, resuspended in DPBS, and used for each round of selection. In the first round, VACV was incubated in 100 μL of DPBS containing 1 μM (0.1 nmol or 6×10^{13} molecules) ssDNA library for 30 min at 25 °C and then centrifuged at 10 000*g* for 10 min at 15 °C, to remove unbound aptamers, followed by rinsing twice with DPBS. Additionally, vials were changed after each centrifugation cycle to remove nonspecific aptamers bound to the plastic wall of the vials. Next, VACV was resuspended in 35 μL of 10 mM Tris−HCl buffer containing 10 mM EDTA, pH 7.4 (TE) buffer (Integrated DNA Technologies, USA), and heated for 10 min at 95 °C, to release the aptamers bound to the virus. After the denaturing step, the viral debris was removed by centrifugation at 14 000*g* for 15 min at 4 °C and the supernatant, which contains the aptamers, was collected and stored at −20 °C before the following PCR amplification.

Virus-bound aptamers were amplified using symmetric and asymmetric PCR cycles, respectively. For the symmetric PCR, 5 μL of the aptamer pool in TE buffer was mixed with 45 μL of symmetric PCR Master Mix, containing the following reagents in the final concentrations: 1× PCR buffer (Promega Corporation, USA), 2.5 mM $MgCl_2$, 0.028 U μL^{-1} GoTaq Hot Start Polymerase (Promega Corporation, USA), 220 μM dNTPs, 500 nM forward primer (5′-CTC CTC TGA CTG TAA CCA CG-3′), and 500 nM reverse primer (5′-GGC TTC TGG ACT ACC TAT GC-3′). Afterward, asymmetric PCR was performed where 5 μL of the symmetric PCR product in TE buffer was mixed with 45 μL of the asymmetric PCR Master Mix containing the same reagents as above, except 1 μM forward Alexa-488 primer (5′-Alexa488-CTC CTC TGA CTG TAA CCA CG-3′) and 50 nM reverse primer. Amplification was performed using the following PCR program: preheating for 2 min at 95 °C, 15 cycles for symmetric PCR or 10−15 cycles for asymmetric PCR of 30 s each at 95 °C, 15 s at 56.3 °C, 15 s at 72 °C, and held at 4 °C. Furthermore, the number of cycles for asymmetric PCR was optimized after each round of aptamer selection, according to the gel electrophoresis results, to avoid side products and to obtain the highest amount of product from the asymmetric PCR round. Afterward, the fluorescently labeled ssDNA was separated from the PCR mixture, primers, and dNTPs with 30 kDa cutoff filters (Nanosep, PALL, USA) by centrifugation at 3800*g* for 13 min at 15 °C followed by 3 times washing with 200 μL of the DPBS buffer. The purification quality was controlled using 3% agar gel electrophoresis. Subsequently, the purified aptamer pool was diluted in 100 μL of DPBS, and its concentration was measured by a NanoDrop-2000 UV−vis spectrophotometer (NanoDrop, USA) and then stored at −20 °C before continuation to the next round. Finally, 100 nM of the evolved aptamer pool was utilized for the next round of selection. Nine more rounds were performed by repeating five steps as described above: (i) incubation of VACV with an aptamer pool from the previous round, (ii) partitioning of bound aptamers from unbound DNA, (iii) elimination of vial-binding DNA, (iv) heat extraction of bound aptamers, and (v) PCR amplification.

For future in vivo applications of these aptamers, two more negative rounds were performed against human and mouse blood cells and plasma and heat-deactivated VACV, as described elsewhere.[31] Briefly, each round consisted of several steps. First, the eighth aptamer pool was incubated with heat-treated VACV at 37 °C for 30 min, and the supernatant was collected after centrifugation at 14 000*g* for 15 min. Second, DNA sequences in the supernatant were incubated with human and mouse blood cells for 30 min at 37 °C and collected again after centrifugation. In the third step, unbound aptamers were incubated with human blood plasma for 5 min and then VACV was added directly to this mixture, incubated for another 15 min, and centrifuged to collect aptamers bound to intact VACV.

Flow Cytometric Analysis. The affinity of the evolved aptamer pools toward VACV was measured using a FC-500 flow cytometer (Beckman Coulter Inc., USA). Virus particles, 1

dx.doi.org/10.1021/ac300047c | Anal. Chem. 2012, 84, 2548−2556

$\times 10^7$ PFU, were preincubated for 20 min at room temperature with 0.1 mg mL^{-1} yeast RNA, as a masking single-stranded nucleic acid, to suppress the nonspecific binding. Afterward, the virus particles were incubated with 100 nM purified Alexa-488-labeled aptamer pool in 50 μL of DPBS buffer for 30 min at 37 °C. Control experiments were performed using the fluorescently labeled ssDNA library in DPBS. Subsequently, each sample was washed once with 200 mL of DPBS to remove the unbound DNA, resuspended in 0.5 mL of DPBS, and subjected to the flow cytometric analysis.

Cloning and Sequencing of the Aptamer Pool. The 12th aptamer pool showing the highest affinity to VACV, according to the flow cytometric data, was cloned. Briefly, the dsDNA pool was extracted from the gel using a DNA gel extraction kit, Axy prep (AxyGen Biosciences, USA), in order to purify the DNA from the PCR mix. Cloning was performed according to the supplied protocol using an M13mp18 Perfectly Blunt Cloning Kit (Novagen, Germany). White colonies were collected into separate tubes, left to grow overnight in 1 mL of SOC medium (Cellgro, USA) at 37 °C and then analyzed by PCR and 3% agar gel electrophoresis to ensure that the clones have the correct insert in their plasmids. For each PCR reaction, 2 μL of the cell suspension was mixed with 18 μL of the PCR Master Mix containing: 1× PCR buffer B, 2.5 mM $MgCl_2$ (Mallinckrodt Baker, Inc., USA), 0.01 U μL^{-1} KAPA 2G Robust Hot Start DNA polymerase (Kapa Biosystems, USA), 220 μM dNTPs, 0.5 μM forward 5′-Alexa-488-labeled primer, and 0.5 μM reverse primer. Amplification was performed using a PCR program (preheating for 5 min at 95 °C, 25−30 cycles of 30 s each at 95 °C, 15 s at 56.3 °C, 15 s at 72 °C, and held at 4 °C). Plasmids were isolated using GeneJET plasmid miniprep kit (Fermentas, USA), according to the supplied protocol. The part of the plasmid with the insert was amplified using M13 forward primer (5′-GTA AAA CGA CGG CCA GT-3′) and M13 reverse primer (5′-AGC GGA TAA CAA TTT CAC ACA GG-3′), according to the following protocol. For each PCR reaction, 5 μL of the plasmid (~10 ng μL^{-1}) diluted in water was mixed with 45 μL of the PCR Master Mix containing 1× PCR buffer A, 25 μM $MgCl_2$, 0.01 U μL^{-1} KAPA 2G Robust Hot Start DNA polymerase, 10 mM dNTPs, 0.5 μM forward M13 primer, and 0.5 μM reverse M13 primer. Amplification was performed using the PCR program (preheating for 2 min at 95 °C, 25 cycles of 30 s each at 95 °C, 15 s at 60 °C, 15 s at 72 °C, and held at 4 °C). Finally, the unpurified PCR product was sequenced at McGill University and Génome Québec Innovation Centre, Canada.

Preparation of the Aptasensor. Prior to experiments, the gold microelectrode (25 μm diameter, CH Instruments, TX, USA) was cleaned by oxidation and reduction scanning under basic conditions (scan rate, 2 V s^{-1}; in 0.5 M NaOH) over the potential range −0.35 to −1.35 V (vs Ag/AgCl reference electrode saturated with 3 M NaCl). Next, the electrode was cyclically cleaned under acidic conditions (scan rate, 4 V s^{-1}; in 0.5 M H_2SO_4) over the same potential range. The scan was typically repeated 1000 times under basic conditions and 100 times under acidic conditions. Afterward, the electrode was cleaned by sonication in absolute ethanol and dried with N_2. Subsequently, the electrode was incubated with equimolar amounts (200 nM) of the aptamer pool and an HPLC purified 5′-/5ThioMC6-D/GGC TTC TGG ACT ACC TAT GC-3′ modified at the 5′ position with a 6-hydroxyhexyl disulfide group, detection probe (Integrated DNA Technologies, USA) in 20 mM Tris−ClO_4 buffer, pH 8.6, for 5 days at 4 °C. Finally, the electrode was incubated with 1 mM 2-mercaptoethanol in ethanol for 5 min to backfill the empty spots of the electrode surface, thus reducing the nonspecific adsorption onto the surface.

Electrochemical Measurements. Electrochemical studies, including cyclic voltammetry (CV) and electrochemical impedance spectroscopy (EIS), were performed with an electrochemical analyzer (CH Instruments 660D, TX, USA) connected to a personal computer. All measurements were carried out at room temperature in an enclosed and grounded Faraday cage. A conventional three-electrode system was used: an anti-VACV aptamer-modified gold electrode as a working electrode, a platinum wire as a counter electrode, and Ag/AgCl/3 M NaCl as a reference electrode. The reference electrode was always isolated from the cell by a miniature salt bridge (agar plus KNO_3) to avoid the leakage of the Cl^- ions from the reference electrode to the measurement system. The open-circuit or rest-potential of the system was measured prior to all electrochemical experiments to prevent sudden potential-related changes in the self-assembled monolayer. CV experiments were performed at a scan rate of 100 mV s^{-1} in the potential range from −200 to 600 mV. EIS measurements were conducted in the frequency range of 100 kHz to 0.1 Hz, at a formal potential of 250 mV and AC amplitude of 5 mV. The measured EIS spectra were analyzed with the help of equivalent circuit using ZSimpWin 3.22 (Princeton Applied Research, USA), and the data were presented in Nyquist plots. All electrochemical measurements were performed in 20 mM Tris−ClO_4 buffer (pH 8.6), containing 2.5 mM $[Fe(CN)_6]^{3-/4-}$. Importantly, all measurements were repeated for a minimum of three times with separate electrodes to obtain statistically meaningful results.

RESULTS AND DISCUSSION

Selection of Anti-VACV Aptamers. Aptamer selection to viruses using cell-SELEX includes two major parts.[30,31] In the first part, ten combined rounds of positive selection to intact VACV and negative selection to plastic vials at 37 °C were carried out as illustrated in Figure 2. The binding affinities of ten aptamer pools were measured by flow cytometry (Figure 3A), and the eighth pool, exhibiting the highest binding affinity to VACV, was chosen for the second part of the selection protocol. To exclude the potential binding of selected aptamers to blood cells and inactive virus, we added two more rounds of negative selection to human and mouse blood cells and heat-deactivated VACV. Additionally, the aptamers were incubated with intact VACV in the presence of blood plasma to retain the most nuclease-resistant aptamers. A small improvement in the binding affinity was observed after these two rounds of negative selection. The fluorescently labeled DNA library was used as a control (Figure 3A). The 12th aptamer pool with the highest binding affinity (EC_{50} = 25 nM) was cloned in *E. coli*, and 50 bacterial colonies containing the aptamer insert were sequenced. After grouping and eliminating repeats, 27 unique clones were analyzed by flow cytometry. The representative flow cytometry assays of the 12th pool, vac2 clone, and DNA library are shown in Figure S2, Supporting Information. All 27 sequences are also provided in Table S1, Supporting Information. Finally, seven aptamer clones (vac1, vac2, vac4, vac5, vac6, vac14, and vac46) with the highest affinities to VACV (Figure 3B) were further utilized in the development of aptasensors and electrochemical differentiation of epitope-specific aptamers.

dx.doi.org/10.1021/ac300047c | *Anal. Chem.* 2012, 84, 2548−2556

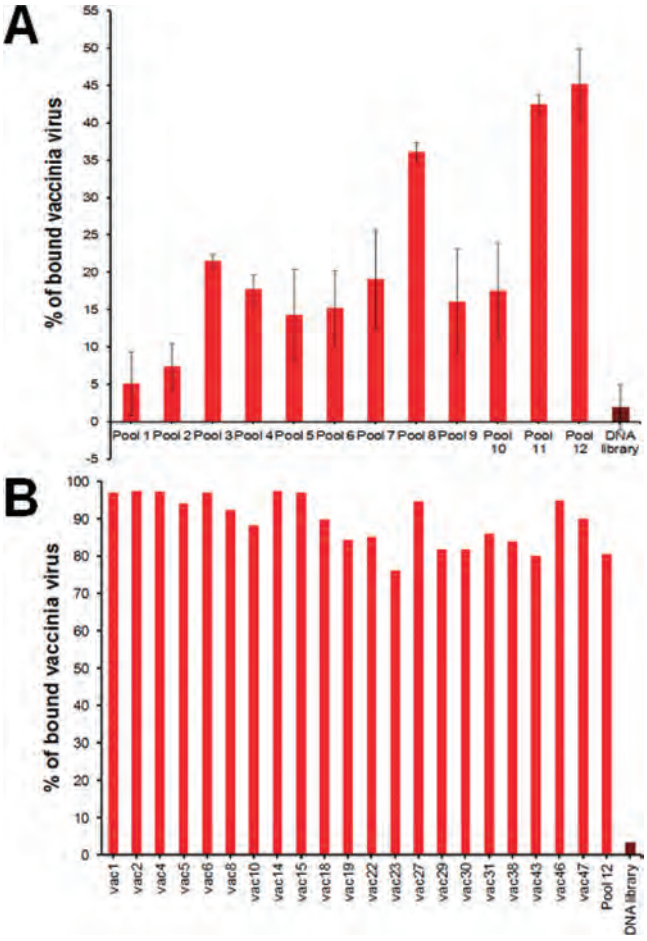

Figure 3. Flow cytometric analysis of binding affinities between 1×10^7 PFU of VACV and 100 nM Alexa-488-labeled aptamer pools (A) and clones (B).

Electrochemical Characterization and Analytical Parameters of the VACV Aptasensor. The electrochemical characteristics of the developed aptasensors were investigated by both cyclic voltammetry (CV) and impedance spectroscopy (EIS). The pretreated gold electrode presents a quasi-reversible voltammogram indicating that the redox reactions easily occurred on the bare gold surface, evidenced by very large redox currents (curve a) as shown in Figure 4A. Formation of SAM of the thiolated primer (a capture probe) terminated with the anti-VACV aptamer (a detection probe) on the gold surface substantially reduced the electrode current, indicating the formation of a highly compact layer. The concentration of the capture strand/aptamer (200 nM) was optimized to prevent cross-hybridization between neighboring aptamers as a result of the self-complementary nature of the individual aptamer sequences. Repulsion between the negatively charged DNA backbone and the redox probe, $[Fe(CN)_6]^{3-/4-}$, is responsible for the significant reduction of the redox currents. Final treatment with 2-mercaptoethanol slightly reduced the redox currents because they can penetrate down to the electrode surface, thereby blocking the direct access of the conducting ions (curve c). The thiol group of the backfilling agent can effectively displace the weaker adsorption contacts between the aptamer nucleotides and the gold surface, leaving the capture probe tethered primarily through the thiol end group. Such conformation improves the flexibility of the probe and renders it more accessible to the target molecules. Moreover, displacement of the nonspecific adsorption provides free volume into the film, which enhances the transport of counterions and solvent molecules through the modified film.[34]

The Nyquist plots of the impedance spectra are shown in Figure 4B and support the CV data. The complex impedance was presented as the sum of the real Z, Z_{re}, and imaginary Z, Z_{im}, components that originate mainly from the resistance and capacitance of the cell, respectively. A suitable equivalent circuit, shown in the inset of Figure 4B, was carefully selected to reflect the real electrochemical process and to enable fit producing accurate values. The circuit is based on the Vorotyntsev theoretical model of a surface confined system that takes into account the charge transfer process at the film/electrolyte interface as well as through film/electrode interface.[35] The circuit consists of the ohmic resistance, R_S, of the electrolyte solution, electrolyte/film interface resistance, R_{ef}, and capacity, CPE_{ef} (used as constant phase element, CPE, a nonlinear capacitor to improve the fitting of experimental data), film resistance, R_f, and capacity, CPE_f, and the Warburg impedance, Z_w, resulting from diffusion of the redox probe. The diameter of the semicircle corresponds to the interfacial resistance at the electrode surface, the value of which depends on the dielectric and insulating features of the surface layer. The low frequency loop observed at the end of the semicircle can be attributed to the Warburg impedance, resulting from a diffusion-limited electrochemical process, presumably due to molecular motions within the film caused by conducting ions penetration[36] as shown in Figure 4B and Table S2, Supporting Information. The interfacial resistance increased after each step of aptasensor preparation, indicating a purely geometric effect on the surface. Interestingly, the self-assembly of the aptamers onto the electrode surface gave 89% (865.7 Ω cm) of the interfacial resistance, assuming that 100% of the resistance was achieved after surface backfilling. This indicates the formation of a compact layer of aptamers and the high quality packing of the surface.

According to flow cytometry data, the 12th aptamer pool showed the highest affinity to VACV and thus was utilized for the preparation of the VACV aptasensor. Prior to titration experiments, aliquots containing different number of VACV particles (500, 1000, 1500, 2000, 2500, 3000 plaque-forming unit or PFU) in 20 μL of Dulbecco's phosphate buffered saline were incubated with the aptasensor at 37 °C for 1 h. EIS was performed, and the numerical values for the circuit components were extracted at each aliquot as shown in Figure 4C and Table S3, Supporting Information. It was observed that the electrolyte ohmic resistance, R_s, which is dependent on the ionic strength of the buffer, dominates at the highest frequency (100 kHz), and thus, it is not affected by the binding reaction of VACV to the immobilized aptamer. Also, the values of R_{ef} and CPE_{ef} did not significantly change after the binding of VACV, which means that the VACV−aptamer complex on the electrode surface does not affect the impedance of film/electrode interface. It was also observed that the R_{ef} value decreases linearly with increasing the number of VACV particles, in the range from 500 to 3000 PFU, with the regression equation of $y = -0.2014x + 856.45$ ($R^2 = 0.954$), where y is the R_{ef} value in Ω cm^2 and x is the number of virus particles in PFU, as shown in Figure 4D. This could be attributed to a conformational change in the aptamers after binding to VACV which allows the external redox mediator to penetrate more freely to the electrode surface.[37] This observation is supported by the

dx.doi.org/10.1021/ac300047c | Anal. Chem. 2012, 84, 2548−2556

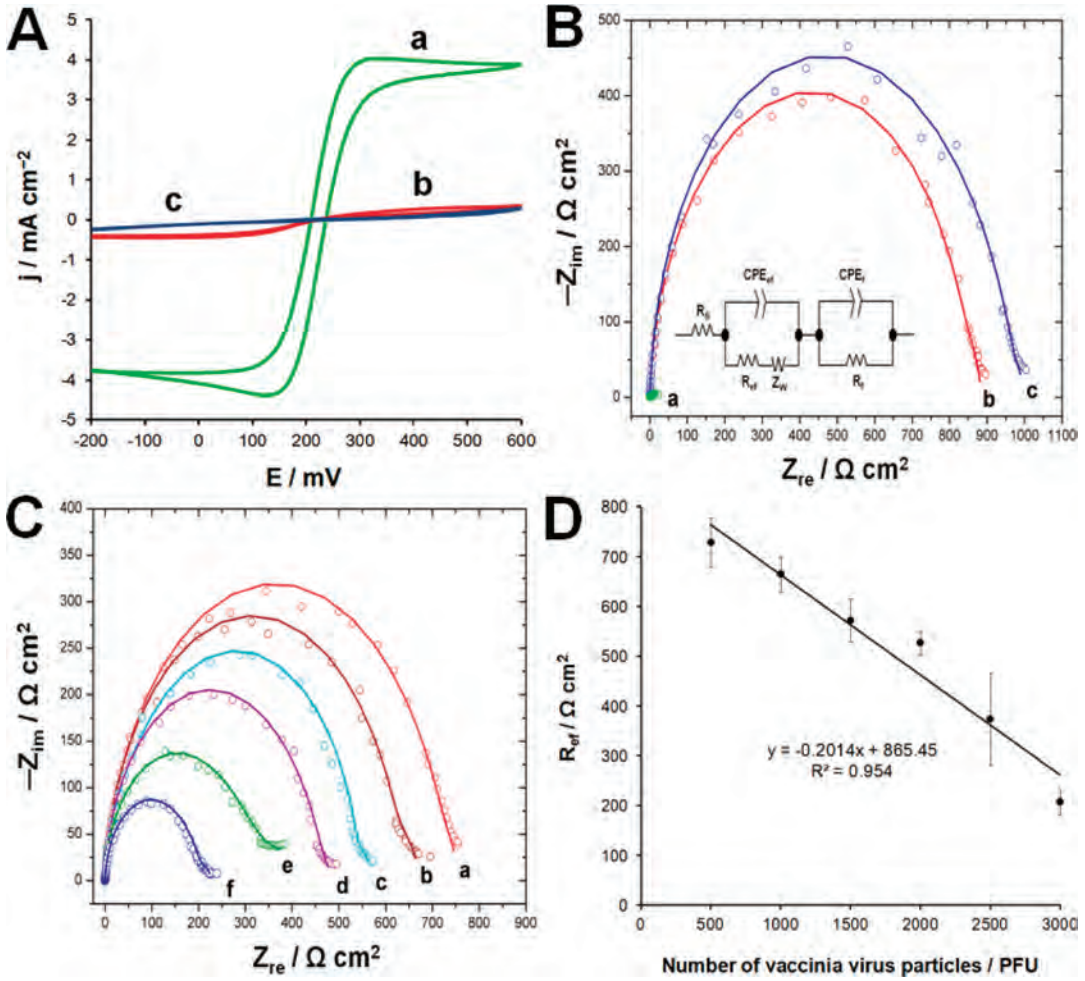

Figure 4. (A) Cyclic voltammograms and (B) Nyquist plot ($-Z_{im}$ vs Z_{re}) of impedance spectra of the VACV aptsensor after each immobilization or binding step. Cyclic voltammograms were recorded at a scan rate of 100 mV s^{-1} for (a) bare gold, (b) after coating with the hybridization product of thiolated primer and VACV-specific aptamer, and (c) after backfilling with 1 mM 2-mercaptoethanol. The inset of (B) represents the circuit employed to fit to EIS measured data. The circuit consists of the ohmic resistance, R_S, of the electrolyte solution, electrolyte/film interface resistance, R_{ef}, and capacity, CPE_{ef}, film resistance, R_f, and capacity, CPE_f, and the Warburg impedance, Z_w, resulting from diffusion of the redox probe. (C) Nyquist plot ($-Z_{im}$ vs Z_{re}) of impedance spectra obtained using (a) 500, (b) 1000, (c) 1500, (d) 2000, (e) 2500, and (f) 3000 PFU of VACV in DPBS after incubation with the developed aptasensor for 1 h at 37 °C. The impedance spectra were recorded from 100 kHz to 0.1 Hz, and the amplitude was 0.25 V vs Ag/AgCl. (D) Calibration plot of R_{ef} vs number of VACV particles. Electrochemical measurements were performed in 20 mM Tris−ClO_4 buffer (pH 8.6), containing 2.5 mM $K_4[Fe(CN)_6]$ and 2.5 mM $K_3[Fe(CN)_6]$.

previous electrochemical characterization of the aptamer film. The relative standard deviation (RSD) values were between 4.4 and 24.7%. Beyond the upper VACV number of particles level, the response became nonlinear, indicating the saturation of the surface with VACV. The limit of detection (LOD) was 330 PFU, estimated from $3(S_b/m)$, where S_b is the standard deviation of the measurement signal for the blank and m is the slope of the analytical curve in the linear region.[38]

The selectivity and cross-reactivity of the developed aptasensor was tested on nonviable heat-treated VACV and vesicular stomatitis virus (VSV) as shown in Figure 5A,B. The nonviable VACV after heating for 30 min at 90 °C caused only 14% decrease in R_{ef} when compared with a buffer control (0%) and 3000 PFU of viable VACV (100%). The sensor was also tested using 3000 PFU of VSV instead of VACV, and it resulted in 12% decrease in R_{ef}. Furthermore, an aptasensor utilizing the native DNA library (instead of the anti-VACV aptamer) caused a 15% increase in R_{ef}. In addition, the specificity of the sensor was tested with 5.1 mg mL^{-1} human serum albumin (HSA, Sigma-Aldrich, USA) which caused a 2% increase in R_{ef}. Flow cytometry experiments also confirmed a good binding of 100 nM aptamers to the viable VACV (79% of 10^5 viruses formed a complex with aptamers) compared to the heat-inactivated VACV (only 13%) and mouse blood cells (0.2%) as seen in Figure S3, Supporting Information.

Affinity Analysis of the Selected Aptamer Clones. Seven aptamer clones were used for the preparation of aptasensors for detection of a fixed number of VACV particles (2000 PFU in 20 μL) by incubation for 1 h at 37 °C. Additionally, two control experiments were performed using the original aptamer pool #12 as well as the DNA library as a nonspecific detection probe. To ensure accuracy, EIS was performed before and after VACV binding to guard against any possible variations in the baseline interfacial resistance values that might be caused by the heterogeneous aptamer clones adopting different conformations on the electrode surface, thereby affecting the ions penetration through the formed film. The electrolyte/film resistance baseline, Rb_{ef}, and after virus binding, Rv_{ef}, were measured, and ΔRv_{ef} was calculated from the formula: $\Delta Rv_{ef} = Rv_{ef} - Rb_{ef}$. The value of ΔRv_{ef} is

dx.doi.org/10.1021/ac300047c | Anal. Chem. 2012, 84, 2548−2556

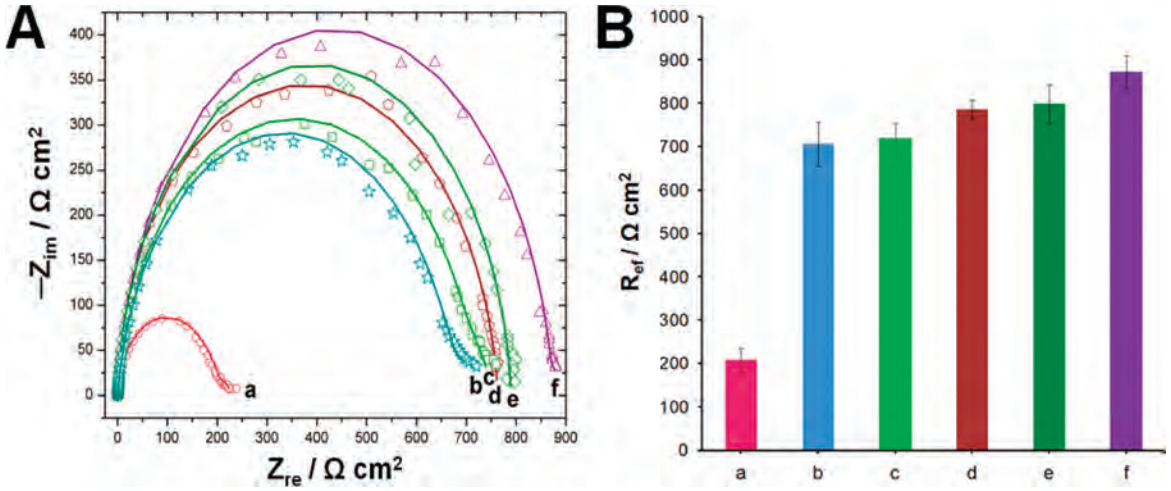

Figure 5. (A) Nyquist plot ($-Z_{im}$ vs Z_{re}) of impedance spectra of the of the selectivity experiments performed using (a) 3000 PFU of VACV, (b) heat-treated 3000 PFU of VACV for 30 min at 90 °C, (c) 3000 PFU of vesicular stomatitis virus (VSV), (d) buffer alone, (e) 5.1 mg mL^{-1} HSA, and (f) 3000 PFU of VACV using DNA library instead of the anti-VACV aptamer pool. All were used in DPBS after incubation with the developed aptasensor for 1 h at 37 °C. The impedance spectra were recorded from 100 kHz to 0.1 Hz, and the amplitude was 0.25 V vs. Ag/AgCl using 20 mM $TrisClO_4$ buffer (pH 8.6), containing 2.5 mM $K_4Fe(CN)_6$ and 2.5 mM $K_3Fe(CN)_6$. (B) A histogram of R_{ef} values for different tested analytes.

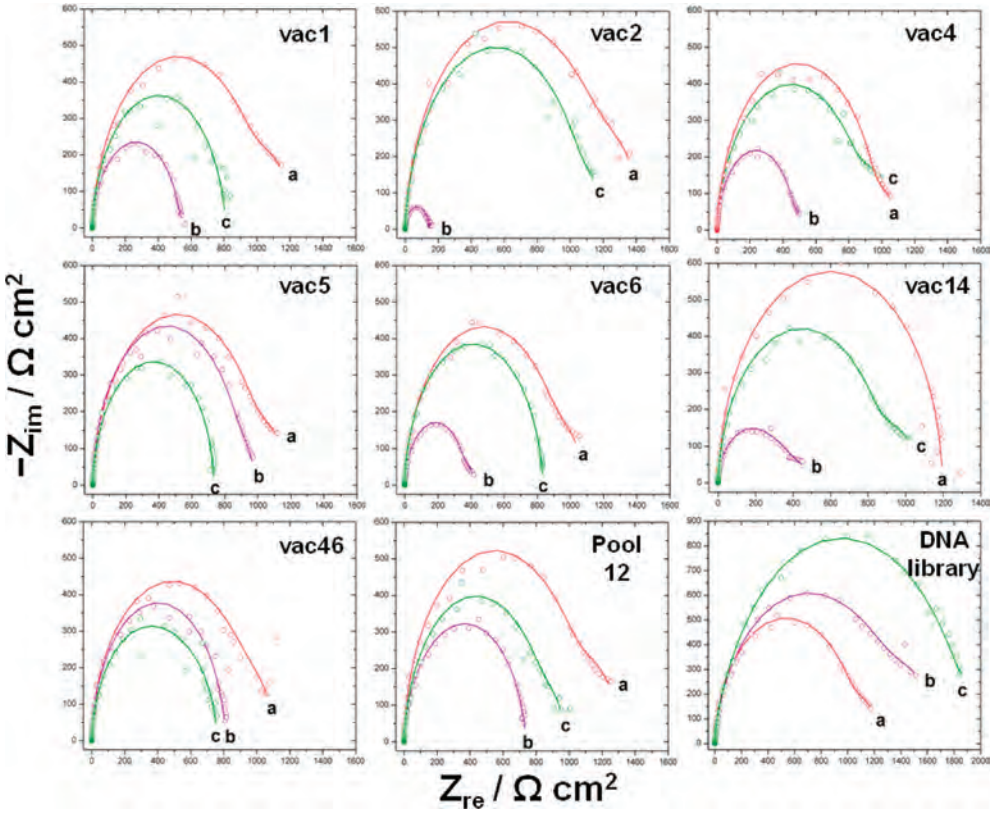

Figure 6. Nyquist plot ($-Z_{im}$ vs Z_{re}) of impedance spectra of VACV aptasensors based on 7 aptamer clones (vac1→vac46) obtained (a) after aptasensor preparation, (b) after binding of 2000 PFU of VACV, and (c) after introduction of 1.0 μg mL^{-1} anti-L1R neutralizing antibody. Two control experiments were performed, under the same conditions, using the original aptamer pool and the native DNA library as a nonspecific detection probe. The impedance spectra were recorded from 100 kHz to 0.1 Hz, and the amplitude was 0.25 V vs Ag/AgCl using 20 mM Tris−ClO_4 buffer (pH 8.6), containing 2.5 mM $K_4[Fe(CN)_6]$ and 2.5 mM $K_3[Fe(CN)_6]$.

indicative of the affinity of the developed aptamer to the virus when the number of virus particles lies within the linear range previously determined in the previous section. The affinities of the aptamers can be ranked as vac2 > vac14 > vac6 > vac4 > vac1 > Pool12 > vac46 > vac5 as shown in Figure 6 and Figure S1 and Table S4, Supporting Information. The results agree well with those obtained using the flow cytometric analysis, as can be seen in Figure 3B.

However, the flow cytometric analysis is less sensitive in distinguishing affinities between different aptamer clones due to the small size of virus particles (360 × 270 × 250 nm). On the other hand, electrochemical sensing allows a better resolution

dx.doi.org/10.1021/ac300047c | *Anal. Chem.* 2012, 84, 2548−2556

Table 1. DNA Sequences and Degree of Protection (DoP) Values of Aptamer Clones Isolated from the 12th Pool[a]

clone	sequence	degree of protection, DoP (%)[b]
vac1	F-CGCGCCCCCGCTGTTCGAGCCGATAGAGGGCTAGTGTCAT-cR	45.9
vac2	F-GTCCGTCCTCTCTCGTTTGTTCCTCTTCTCTTATCTGTCA-cR	86.9
vac4	F-GATTTCCCAGATCCAATTCAAGTCTCAATATCTACCTCA-cR	92.5
vac5	F-CTAGTGCCCCTCTTGTCATCATCTGTTGTTATCTGCCTGG-cR	−209.4
vac6	F-GTGAGGGTCCTGTGGTTGGTGTGGTTGGTGAGATGTGGTGG-cR	79.2
vac14	F-CCATCACCCTATTATCTCATTATCTCGTTTTCCCTATGCG-cR	68.6
vac46	F-CGGGATGTAATACATTTCAGTGTTGGGACCGTACA-cR	−67.9

[a]Where F: CTC CTC TGA CTG TAA CCA CG (the forward PCR primer) and cR: GCA TAG GTA GTC CAG AAG CC (the reverse-complement of the reverse PCR primer). [b]DoP is calculated from the formula DoP = $(\Delta Rv_{ef} - \Delta Ra_{ef})/\Delta Rv_{ef}$ (%).

in comparing binding affinities of different aptamers. Some aptamer clones exhibited higher affinities toward VACV compared to the 12th pool. This could be explained by the heterogeneous nature of the aptamer pool (a polyclonal pool) which consists of a mixture of monoclonal aptamers. Interestingly, the binding of VACV to the DNA library caused an increase in impedance of the aptasensor. This indicates that the binding of VACV does not change the conformation of the immobilized nonspecific DNA; instead, it increases the electrolyte/film interfacial resistance.

Electrochemical Differentiation of Epitope-Specific Aptamers. An electrochemical displacement assay was performed to ensure that the selected aptamer clones can protect the virus from nAbs and, thereby, enhance the in vivo survival of the oncolytic virus. The previously mentioned clones were immobilized onto the gold electrodes, incubated with VACV and washed to remove the unbound virus. Then, the aptasensor was incubated with a high concentration (1.0 μg mL^{-1}) of L1R protein-specific monoclonal antibody (BEI Resources, USA) for 1 h at 37 °C. Two control experiments were carried out, including the aptamer pool #12 and the native DNA library. The introduction of the anti-VACV antibody caused an increase (shift-back) in the interfacial resistance for clones vac1, vac2, vac4, vac6, vac14, and the 12th pool as seen in Figures 6 and S1, Supporting Information. This could be explained by the competitive binding of the antibody to VACV with the subsequent dissociation of the aptamer−virus complex. Release of the virus particles indicates that the aptamers bind to the L1R protein, the main target of neutralizing antibodies.[13,17] Interestingly, two aptamer sequences, vac5 and vac46, showed a decrease in the interfacial resistance upon antibody binding. It indicates that L1R antibody binds to different epitopes other than the one occupied by the aptamer on the surface of VACV without dissociating the aptamer−virus complex.

The difference between the signals after adding nAb and after adding VACV to the aptasensor could be used to estimate the degree of protection (DoP) of VACV by the selected aptamers. This can be calculated from the formula: DoP = $(\Delta Rv_{ef} - \Delta Ra_{ef})/\Delta Rv_{ef}$ (%), where ΔRv_{ef} and ΔRa_{ef} represent the difference between the electrolyte/film interface resistance before and after introduction of nAb, respectively, as shown in Table S4, Supporting Information. The DoP value indicates the affinity of an aptamer to a virus, whereas its sign shows if the aptamer can protect the virus or not. Thus, a positive DoP indicates virus protection from nAb, whereas a negative DoP indicates noncompetitive binding of the aptamer to the virus. The final results of aptamer sequences and DoP values are presented in Table 1.

CONCLUSION

In this work, novel DNA aptamers were raised against the oncolytic vaccinia virus to protect it from neutralizing antibodies. We also developed a multifunctional biosensing platform for quantitative analysis of VACV with an LOD of 330 PFU and electrochemical differentiation of epitope-specific aptamers. Three aptamers, vac2, vac4, and vac6, could bind to the same viral epitope as the L1R-specific antibody (the main neutralizing antibody in blood) and could be applied for aptamer-facilitated virus immunoshielding (AptaVISH).[30] AptaVISH promises to extend plasma circulation time of oncolytic viruses and to provide access to disseminated (metastatic) cancer cells. The risk of decreased virus−cell interactions and anticancer activity due to noncovalently bound aptamers on the surface of virions could be solved by the application of weaker aptamers or injecting an antidote of oligonucleotides with a complementary sequence to the shielding aptamer.[39] The antidote will form a dsDNA helix stable enough to release the virion and let it interact with a target cell. Furthermore, since the aptamers are only present during the initial delivery phase, any nAbs that are developed can help control the viral replication outside of the tumor bed.

Two clones, vac4 and vac46, can bind without protecting the virus from L1R-specific antibody. These aptamers can be utilized either in protecting VACV from other nAbs or for detecting it in a sandwich assay format. The sandwich assay can significantly improve the sensitivity and selectivity of many bioassays and prevent the dissociation of target analytes from their complexes with the capture probes. In addition, both types of aptamers can be used for large scale purification of VACV in virus manufacturing since they are significantly cheaper (∼1000 times) and more stable than antibodies.

The eDEA technology opens a new venue for the production of aptamers to viral and many other epitopes at their native state and conformation. Hence, this technology surpasses the limitations of many conventional methods for development of aptamers against recombinant proteins which may not possess the native folding and post-translational modifications.

ASSOCIATED CONTENT

Supporting Information

Additional information as noted in text. This material is available free of charge via the Internet at http://pubs.acs.org.

AUTHOR INFORMATION

Corresponding Author

*E-mail: maxim.berezovski@uottawa.ca. Tel: 613-562-5800 (1898).

Notes

The authors declare no competing financial interest.

■ ACKNOWLEDGMENTS

M.L. and A.S.Z. contributed equally to this work. This work was supported by Strategic Project Grant #396508-10 from the Natural Sciences and Engineering Research Council of Canada (NSERC). Authors thank Mr. Mohamed Wehbe and Mr. Afnan Azizi for critically reviewing the manuscript.

■ REFERENCES

(1) Enserink, M. *Science* **2004**, *306*, 392−394.
(2) Damon, I. In *Fields Virology*; Raven Press Ltd.: New York, 2007, pp 2079−2081.
(3) Lofquist, J. M.; Weimert, N. A.; Hayney, M. S. *Am. J. Health-Syst. Pharm.* **2003**, *60*, 749−756.
(4) Whitley, R. J. *Antiviral Res.* **2003**, *57*, 7−12.
(5) Breitbach, C. J.; Burke, J.; Jonker, D.; Stephenson, J.; Haas, A. R.; Chow, L. Q.; Nieva, J.; Hwang, T. H.; Moon, A.; Patt, R.; Pelusio, A.; Le Boeuf, F.; Burns, J.; Evgin, L.; De Silva, N.; Cvancic, S.; Robertson, T.; Je, J. E.; Lee, Y. S.; Parato, K.; Diallo, J. S.; Fenster, A.; Daneshmand, M.; Bell, J. C.; Kirn, D. H. *Nature* **2011**, *477*, 99−102.
(6) Goebel, S. J.; Johnson, G. P.; Perkus, M. E.; Davis, S. W.; Winslow, J. P.; Paoletti, E. *Virology* **1990**, *179*, 247−266.
(7) Yu, Y. A.; Shabahang, S.; Timiryasova, T. M.; Zhang, Q.; Beltz, R.; Gentschev, I.; Goebel, W.; Szalay, A. A. *Nat. Biotechnol.* **2004**, *22*, 313−320.
(8) Fisher, K. D.; Seymour, L. W. *Adv. Drug Delivery Rev.* **2010**, *62*, 240−245.
(9) Doronin, K.; Shashkova, E. V.; May, S. M.; Hofherr, S. E.; Barry, M. A. *Hum. Gene Ther.* **2009**, *20*, 975−988.
(10) Ong, H. T.; Hasegawa, K.; Dietz, A. B.; Russell, S. J.; Peng, K. W. *Gene Ther.* **2007**, *14*, 324−333.
(11) Condit, R. C.; Moussatche, N.; Traktman, P. *Adv. Virus Res.* **2006**, *66*, 31−124.
(12) Rodriguez, J. F.; Janeczko, R.; Esteban, M. *J. Virol.* **1985**, *56*, 482−488.
(13) Wolffe, E. J.; Vijaya, S.; Moss, B. *Virology* **1995**, *211*, 53−63.
(14) Hsiao, J. C.; Chung, C. S.; Chang, W. *J. Virol.* **1999**, *73*, 8750−8761.
(15) Davies, D. H.; McCausland, M. M.; Valdez, C.; Huynh, D.; Hernandez, J. E.; Mu, Y.; Hirst, S.; Villarreal, L.; Felgner, P. L.; Crotty, S. *J. Virol.* **2005**, *79*, 11724−11733.
(16) Nelson, G. E.; Sisler, J. R.; Chandran, D.; Moss, B. *Virology* **2008**, *380*, 394−401.
(17) Hooper, J. W.; Custer, D. M.; Schmaljohn, C. S.; Schmaljohn, A. L. *Virology* **2000**, *266*, 329−339.
(18) Labib, M.; Hedström, M.; Amin, M.; Mattiasson, B. *Anal. Chim. Acta* **2009**, *634*, 255−261.
(19) Labib, M.; Hedström, M.; Amin, M.; Mattiasson, B. *Anal. Bioanal. Chem.* **2009**, *393*, 1539−1544.
(20) Labib, M.; Shipman, P. O.; Martić, S.; Kraatz, H.-B. *Electrochim. Acta* **2011**, *56*, 5122−5128.
(21) Martić, S.; Labib, M.; Kraatz, H. B. *Talanta* **2011**, *85*, 2430−2436.
(22) Martić, S.; Labib, M.; Kraatz, H. B. *Electrochim. Acta* **2011**, *56*, 10676−10682.
(23) Martic, S.; Labib, M.; Kraatz, H. B. *Analyst* **2011**, *136*, 107−112.
(24) Martić, S.; Labib, M.; Freeman, D.; Kraatz, P. H. *Chemistry* **2011**, *17*, 6744−6752.
(25) Labib, M.; Hedström, M.; Amin, M.; Mattiasson, B. *Biotechnol. Bioeng.* **2009**, *104*, 312−320.
(26) Labib, M.; Hedström, M.; Amin, M.; Mattiasson, B. *Anal. Chim. Acta* **2010**, *659*, 194−200.
(27) Labib, M.; Hedström, M.; Amin, M.; Mattiasson, B. *Anal. Bioanal. Chem.* **2010**, *397*, 1217−1224.
(28) Labib, M.; Shipman, P. O.; Martić, S.; Kraatz, H. B. *Analyst* **2011**, *136*, 708−715.
(29) Labib, M.; Martić, S.; Shipman, P. O.; Kraatz, H. B. *Talanta* **2011**, *85*, 770−778.
(30) Labib, M.; Zamay, A. S.; Muharemagic, D.; Chechik, A.; Bell, J. C.; Berezovski, M. V. *Anal. Chem.* **2012**, *84*, 1677−1686.
(31) Labib, M.; Zamay, A. S.; Muharemagic, D.; Chechik, A. V.; Bell, J. C.; Berezovski, M. V. *Anal. Chem.* **2012**, *84*, 1813−1816.
(32) Berezovski, M. V.; Lechmann, M.; Musheev, M. U.; Mak, T. W.; Krylov, S. N. *J. Am. Chem. Soc.* **2008**, *130*, 9137−9143.
(33) Sefah, K.; Shangguan, D.; Xiong, X.; O'Donoghue, M. B.; Tan, W. *Nat. Protoc.* **2010**, *5*, 1169−1185.
(34) Radi, A. E.; Acero Sanchez, J. L.; Baldrich, E.; O'Sullivan, C. K. *J. Am. Chem. Soc.* **2006**, *128*, 117−124.
(35) Vorotyntsev, L. I.; Daikhin, M. D.; Levi, J. *J. Electroanal. Chem.* **1994**, *364*, 37−49.
(36) Baur, J.; Gondran, C.; Holzinger, M.; Defrancq, E.; Perrot, H.; Cosnier, S. *Anal. Chem.* **2010**, *82*, 1066−1072.
(37) Radi, A. E.; O'Sullivan, C. K. *Chem. Commun. (Cambridge, U.K.)* **2006**, 3432−3434.
(38) Bard, A. J.; Faulkner, L. R. *Electrochemical Methods: Fundamental and Applications*; Wiley, New York, 2001.
(39) Rusconi, C. P.; Roberts, J. D.; Pitoc, G. A.; Nimjee, S. M.; White, R. R.; Quick, G. Jr.; Scardino, E.; Fay, W. P.; Sullenger, B. A. *Nat. Biotechnol.* **2004**, *22*, 1423−1428.

Supporting Information

Electrochemical Differentiation of Epitope-specific Aptamers

Mahmoud Labib[a], Anna S. Zamay[a,b], Darija Muharemagic[a], Alexey V. Chechik[a], John C. Bell[c,d], and Maxim V. Berezovski[a*]

[a] Department of Chemistry, University of Ottawa, 10 Marie Curie, Ottawa, Ontario K1N 6N5, Canada; [b]Institute of Molecular Medicine and Pathological Biochemistry, Krasnoyarsk State Medical University, 1 P. Zheleznyaka str., Krasnoyarsk 660022, Russia; [c] Department of Biochemistry, Microbiology and Immunology, Faculty of Medicine, University of Ottawa, 501 Smyth Road, Ottawa, Ontario K1H 8L6, Canada; [d]Jennerex Inc., 450 Sansome Street, 16th floor, San Francisco, California 94111, USA.

*Corresponding author: M.V. Berezovski (maxim.berezovski@uottawa.ca) Tel: 613-562-5600 (1898)

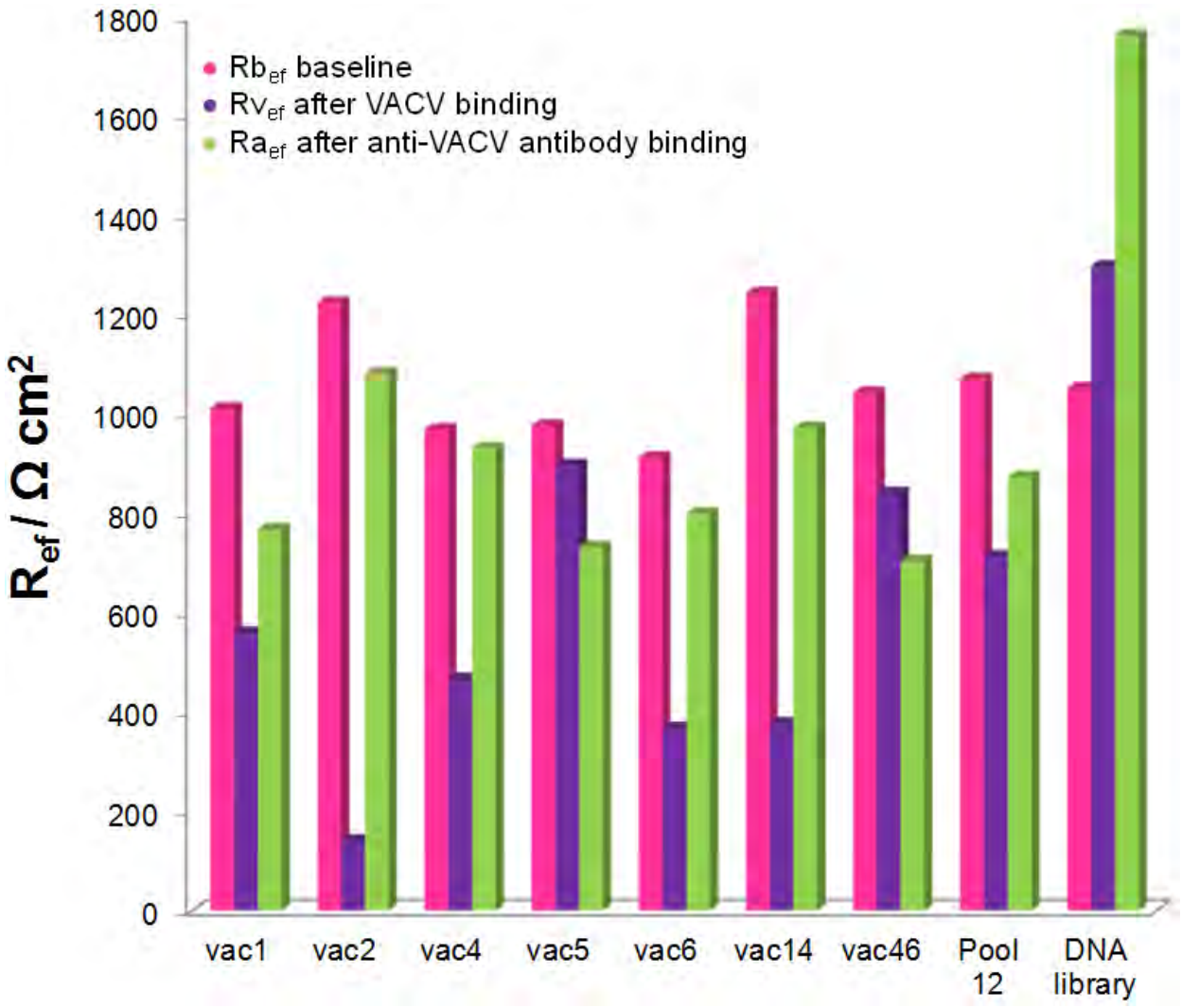

Figure S1. Plot of the electrolyte/film interface resistance, R_{ef}, baseline, after VACV binding (2,000 PFU), and after introduction of the anti-VACV antibody (1.0 µg mL^{-1}). Two control experiments were performed, under the same conditions, using the original aptamer pool and the native DNA library as a non-specific detection probe.

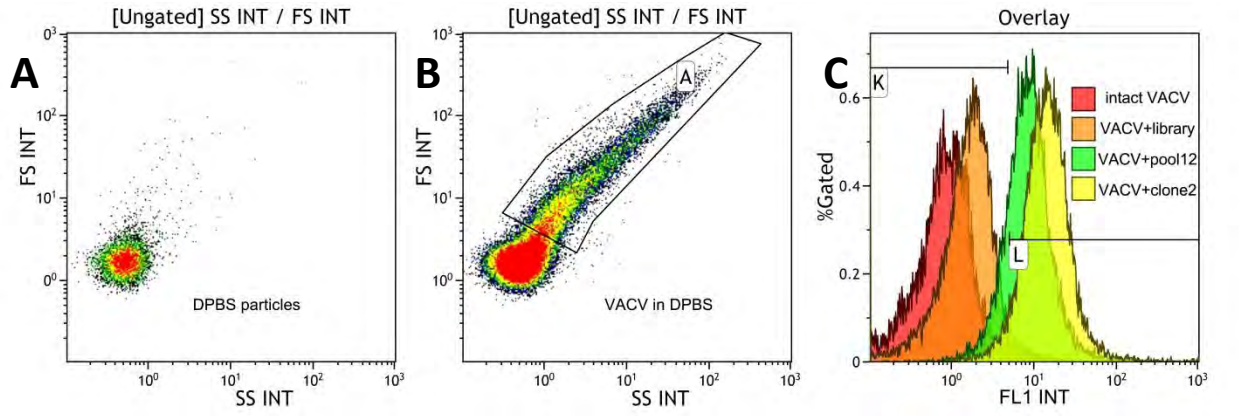

Figure S2. Flow cytometry gating and binding analysis of the native DNA library, the 12th aptamer pool and the aptamer clone (vac2). **(A)** A dot-plot of forward *vs.* side scattering of debris from DPBS buffer; **(B)** Gating of only VACV particles in DPBS (gate A); **(C)** Gated flow cytometric histograms of the binding of 100 nM Alexa-488-labeled native ssDNA library (orange), the aptamer pool #12 (green) and an aptamer clone vac2 (yellow) to 1 × 10^7 PFU of VACV. The percent of bound virus was calculated as the number of counts in Gate L divided by the total number of counts of virus particles in Gate A.

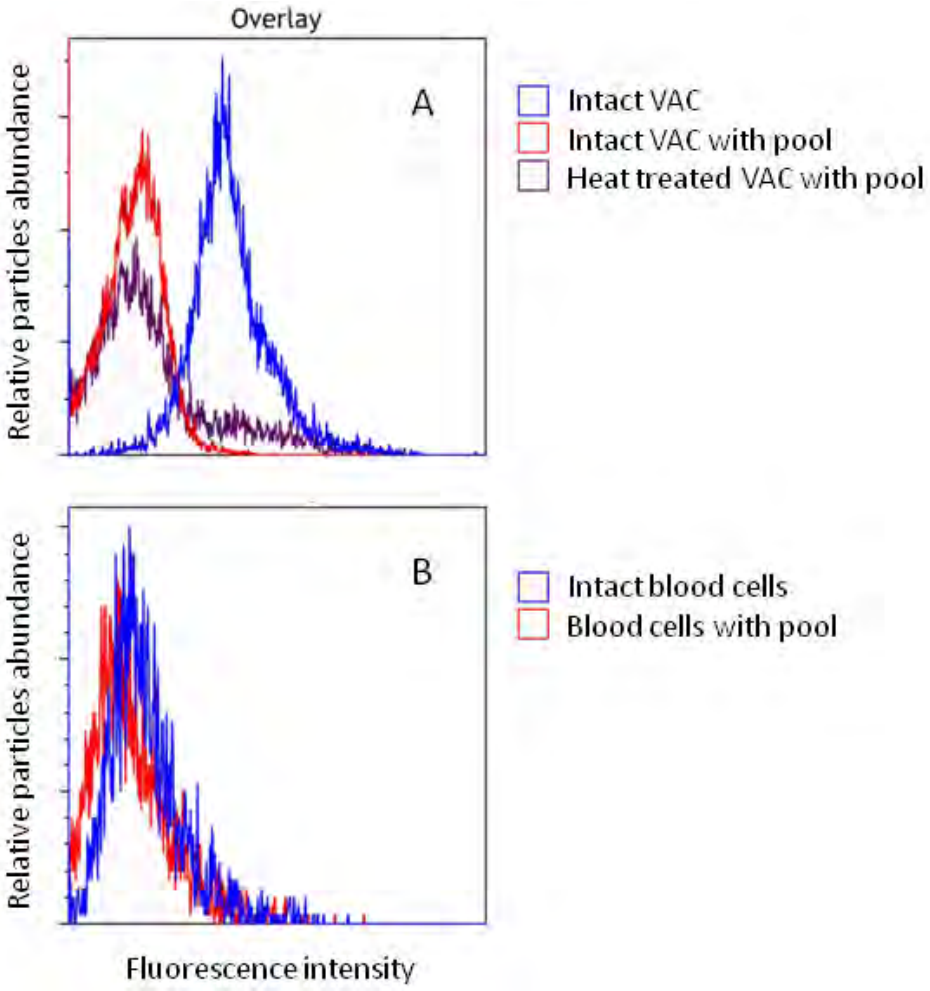

Figure S3. Flow cytometric binding analysis of the Alexa488-labeled pool to viable, heat-inactivated vaccinia virus and mouse blood cells. (A) Histograms of the aptamer pool (100 nM) binding to viable (blue curve) and heat-inactivated vaccinia virus (1×10^5 PFU). Red curve represents the viable virus in absence of the aptamer pool. (B) Histograms of the aptamer pool (100 nM) binding to mouse blood cells. Red curve represents the mouse blood cells in absence of the aptamer pool.

Table S1. Sequences of clones isolated from the 12th pool, where F: CTC CTC TGA CTG TAA CCA CG (the forward PCR primer) and cR: GCA TAG GTA GTC CAG AAG CC (the reverse-complement of the reverse PCR primer).

Clone	*Sequence*
vac1	F─ CGCGCCCCCGCTGTTCGAGCCGATAGAGGGCTAGTGTCAT ─ cR
vac2	F─ GTCCGTCCTCTCTCGTTTGTTCCTCTTCTCTTATCTGTCA─ cR
vac4	F─GATTTCCCAGATCCAATTCAAGTCTCAATATCTACCTCA─ cR
vac5	F─CTAGTGCCCCTCTTGTCATCATCTGTTGTTATCTGCCTGG─ cR
vac6	F─GTGAGGGTCCTGTGGTTGGTGTGGTTGGTGAGATGTGGTGG─ cR
vac8	F─GGCTTACCGTTGCGCAGTGGACTGGAGGATGCCACTTTC─ cR
vac9	F─CCATCACCCTATTATCTCATTATCTCGTTTTCCCTATGCG─ cR
vac10	F─GGGGAGTTTACATAACACGAATTGCGATTACTTCCAGTGG─ cR
vac13	F─GTGCCCAATCCGCGGTTCACTTCTACGTGATGCCCGGCCT─ cR
vac14	F─CCATCACCCTATTATCTCATTATCTCGTTTTCCCTATGCG─ cR
vac15	F─GGCGGTCCCTTCTTTTTGTGTTTATGTTGTTCTCTTTTCG─ cR
vac18	F─CCATCACCCTATTATCTCATTATCTCGTTTTCCCGATGCG─ cR
vac21	F─GCCTAACTAAAGGGTGAAGACAAATTAATTAGGCTTGAAT─ cR
vac22	F─CTAGTGCCCCTCTTGTCATCATCTGTTGTTATCTGCCAGG─ cR
vac23	F─AGCTAGACGTGTTCTGATTGTATGACCATCCTCTCCTTCT─ cR
vac27	F─CGCTTACTTCAATAGGTTATACAAGTGGTTGATTTCCCGTT─ cR
vac29	F─ATCCGACTGACAAGCCGCGAACCTCGGGTTCGTAACGAGA─ cR
vac30	F─TGGTAATCGATGGGATGGATGAATTTTCGTCTGGTGGCCA─ cR
vac31	F─GGCCGGGGAAGTCCGCCAGTTTGGGCCGCAAAGCCATTGA─ cR
vac33	F─CTAGTGCCCCTCTTGTCATCATCTGTTGCTATCTGCCTGG─ cR
vac37	F─TGGCAACATCTCCTCTGACTGTAACCAC─ cR
vac39	F─CTAGTGCCCCTCTTGTCATCATCTGTTGTTATCTGCCTGG─ cR

vac41	F─CCATCACCCTATTATCTCATTATCTCGTTTTCCCTATG─ cR
vac46	F─CGGGATGTAATACATTTCAGTGTTGGGACCGTACA─ cR
vac47	F─ACTCTCCAGATATAACGGCACACCGTTACCTGGGCGTG─ cR

Table S2. Equivalent circuit element values for the VACV aptasensor, after each binding or modification step.

Modification	Rs (Ω cm^2)	CPE_{ef} (μF cm^2)	n_1	R_{ef} (Ω cm^2)	W ($\mu F^{0.5}$ cm^2)	CPE_f (μF cm^2)	n_2	R_f (Ω cm^2)
Bare gold	0.01 (0.002)[a]	44.1 (0.01)	0.91 (0.01)	3.3 (0.6)	425.8 (38.9)	13000 (282.8)	0.56 (0.02)	22.1 (0.47)
After self-assembly of the primer/aptamer	0.03 (0.004)	29.2 (1.1)	0.96 (0.01)	865.7 (62.8)	2.1×10^{-4}(2.83×10^{-4})	71.45 (9.3)	0.96 (0.01)	0.1 (0.02)
After back-filling with 2-mercaptoethanol	0.03 (0.002)	27.4 (1.3)	0.97 (0.01)	969.1 (72.6)	6.93×10^{-8}(9.49×10^{-8})	80.95 (10.5)	0.92 (0.003)	0.1 (0.02)

[a] The values in parentheses represent the standard deviations from at least three electrode measurements.

Table S3. Equivalent circuit element values for the developed VACV aptasensor, in the presence of increasing number of virus particles

Number of virus particles (PFU)	Rs (Ω cm^2)	CPE_{ef} (μF cm^2)	n_1	R_{ef} (Ω cm^2)	W (μF$^{0.5}$ cm^2)	CPE_f (μF cm^2)	n_2	R_f (Ω cm^2)
500	0.03 (0.001)[a]	29.4 (1.8)	0.95 (0.007)	729.5 (49.6)	11 (0.5)	77.21 (47.6)	1 (0)	0.17 (0.02)
1000	0.03 (0.002)	31.6 (1.3)	0.97 (0.01)	665.7 (35.5)	13.59 (1.7)	574.9 (222.2)	0.8 (0.005)	0.34 (0.08)
1500	0.03 (0.002)	34.9 (1.5)	0.94 (0.003)	572.4 (42.9)	39.87 (5.3)	87.1 (69.7)	1 (0)	0.17 (0.03)
2000	0.03 (0.001)	36.5 (0.8)	0.96 (0.003)	528 (23.1)	51.27 (4.7)	38.1 (14.8)	1 (0)	0.15 (0.01)
2500	0.02 (0.001)	41.9 (3.2)	0.96 (0.002)	374.6 (92.4)	61.57 (1.8)	92.5 (13.2)	0.94 (0.001)	0.17 (0.01)
3000	0.03 (0.001)	47.7 (0.9)	0.97 (0.004)	208.3 (26)	139 (10.3)	53.1 (19.6)	1 (0)	0.16 (0.01)

[a] The values in parentheses represent the standard deviations from at least three electrode measurements.

Table S4. Electrolyte/film interface resistance, R_{ef}, baseline after fabrication of the sensor (Rb_{ef}), after vaccinia virus binding (Rv_{ef}), after introduction of the anti-vaccinia antibody (Ra_{ef}), and the degree of protection (*DoP*) of the virus imparted by each of the aptamer clones as well as the original pool. Control experiments were performed using the native DNA library as a non-specific detection probe.

Pool/ Clone	Rb_{ef}	Rv_{ef}	Ra_{ef}	ΔRv_{ef} $(Rv_{ef} - Rb_{ef})$	ΔRa_{ef} $(Ra_{ef} - Rb_{ef})$	*Degree of Protection, DoP,* $(\Delta Rv_{ef} - \Delta Ra_{ef}) / \Delta Rv_{ef}$ *(%)*
vac1	1012	560.9	768	-451.1	-244	45.9
vac2	1224	141.9	1082	-1082.1	-142	86.9
vac4	969.3	467	931.7	-502.3	-37.6	92.5
vac5	976.6	897.6	732.2	-79	-244.4	-209.4
vac6	912.4	367.9	799.4	-544.5	-113	79.2
vac14	1244	377.4	972.1	-866.6	-271.9	68.6
vac46	1043	841.3	704.4	-201.7	-338.6	-67.9
Pool 12	1071	713.9	873	-357.1	-198	44.6
DNA library	1052	1298	1763	246	711	-189